Advances in Science and Technology Research Journal

Advances in Science and Technology Research Journal, 2026, 20(8), 420–429
https://doi.org/10.12913/22998624/221205
ISSN 2299-8624, License CC-BY 4.0

Received: 2026.04.02
Accepted: 2026.06.01
Published: 2026.07.01

Effect of the B stiffness submatrix on the free oscillation of thin-walled plates made of a general laminate

Zbigniew Kolakowski[1], Andrzej Teter[2*]

[1] Department of Strength of Materials (K-12), Lodz University of Technology, ul. Stefanowskiego 1/15, 90-924 Lodz, Poland

[2] Department of Applied Mechanics, Faculty of Mechanical Engineering, Lublin University of Technology, ul. Nadbystrzycka 36, 20-618 Lublin, Poland

* Corresponding author's e-mail: a.teter@pollub.pl

ABSTRACT

This study investigates the lowest natural frequencies of simply supported thin-walled rectangular plates made of laminates with arbitrary stacking sequences. A detailed analysis is made of laminates whose stacking sequences meet the non-zero condition for coupling stiffness submatrix B components. Twelve laminate stacking sequences exhibiting different types of in-plane and out-plane coupling effects are selected, assuming that the plies are of the same thickness. A comparison is made between the effects of selected components of the coupling stiffness submatrix B and inertial force components on the natural frequencies of the rectangular laminate plates under consideration. Classical laminate plate theory (CLPT) is used in the considerations. Obtained solutions of the eigenproblems for the cases of unloaded rectangular plates made of a general laminate show that the correct determination of eigenvalues requires a detailed analysis of all B stiffness matrix components and beam model reduction factors.

Keywords: coupling effects, vibrations, natural frequencies, general laminate, rectangular plate.

INTRODUCTION

Plate structures are widely used in modern lightweight load-bearing structures because they can easily be adapted to complex design requirements. Owing to the widespread use of these structures, it is increasingly important to understand their dynamic behaviour. This is particularly vital in the case of optimized laminate structures made of modern laminates with arbitrary stacking sequences. Modern methods make it possible to considerably change mechanical properties of laminate structures and thus their natural frequencies, which allows for these materials to be tailored to specific applications. Laminates with arbitrary stacking sequences exhibit in-plane and out-plane coupling effects, which poses a significant challenge in terms of their manufacturing. Components made from such laminates often undergo warping. Once installed in a load-bearing structure, they exhibit high initial stresses. Among the laminates with arbitrary stacking sequences, thermally stable laminates, which are insensitive to temperature variations during the manufacturing process, are of particular interest due to their application potential. Their use could prevent the warping of finished plate components and avoid excessive initial stresses.

The problem of natural vibrations of square laminate plates under different boundary conditions was investigated by third-order shear deformation theory (TSDT) in [1]. The determined natural frequencies were compared with results obtained by finite element method (FEM). In [2], a similar problem was solved using radial Gaussian basis functions and first-order shear deformation theory. A monograph [3] proposed a unified accurate method for analysing natural vibrations of laminate beams, plates, and shells with general boundary conditions, including classical edges, elastic supports, and their combinations. The work provided numerous solutions for a variety of configurations, taking into account different boundary conditions, lamination schemes, geometries, and material parameters. In [4], a method was proposed for determining the natural frequencies of arbitrary laminate plates under different boundary conditions, and the effect of the selected number of layers of special orthotropic laminates on the fundamental natural frequency was investigated. A new method for analysing the free vibration and buckling of rectangular orthotropic plates by superposition methods was proposed in [5]. A study [6] presented solutions for the natural frequencies of laminate plates with different combinations of ply orientations, i.e., angle plies and cross plies, up to 21 layers, selected based on current industrial design practice. In another study [7], the same authors presented details of the algorithm used to develop the definitive list of laminate stacking sequences with up to 21 plies, as well as developed natural frequency factor envelopes. A review paper [8] focused on the free vibration of sandwich and laminated composite plates. For the different methods under analysis, the displacement fields of different theories were presented and compared using Navier-type solutions. A total of 391 references were cited. In [9], Hamilton's principle in FSDT was employed to propose a method for free vibration analysis of rectangular laminate composite plates with general stacking sequences and edge restraints, in which the generalized displacements were expanded into series with Lagrange polynomials as basic functions.

In [10] first-order shear theory was utilized to investigate the free vibration behaviour of functionally graded thin, moderately thick, and thick multilayer composite plates reinforced with graphene nanoplatelets (GPLs). The problem was solved by finite element method. The effect of four different layer-wise variations of GPL distribution along the thickness and all possible plate edge boundary condition combinations on the natural frequencies of the plate was investigated. A paper [11] was a FEM numerical and experimental study on the free vibration of woven glass fibre laminate composite stiffened plates. The results showed very good agreement. In [12] an effective vibration analysis and counting theory were used to identify all combinations of boundary conditions for in-plane vibration of symmetrically laminate rectangular plates. In the numerical calculations, all sets of natural frequencies were calculated for the rectangular plates with different aspect ratios, material properties, and lamination.

The static, buckling, and dynamic behaviour of a laminate plate structure with helicoidal orientation scheme was investigated in [13] via first-order shear deformation theory (FSDT). In [14], a four-node quadrilateral plate element was developed for free vibration analysis of laminate composite plates using TSDT. The composite plate element was free from shear locking. The accuracy of the calculated natural frequencies of laminate composite plates was compared with other results. In [15], a theoretical investigation was conducted on the free and forced vibration of carbon/glass hybrid composite laminate plates under arbitrary boundary conditions using FSDT, Lagrange equations, and Rayleigh-Ritz variational operations. The study determined the impact of hybrid ratios, stacking sequences, lamination schemes, fibre orientations, boundary conditions, and excitation force on the free and forced vibration behaviour of the carbon/glass hybrid composite laminate plates.

In [16–18], an analytical method was proposed for determining the vibration characteristics of smart laminate composite plates reinforced with bamboo fibres and integrated with piezoelectric materials. Natural frequencies of the plates were calculated by solving an eigenvalue problem, considering the effects of boundary conditions, piezoelectric materials, fibre volume fraction, stacking sequence, plate geometry, and composite material properties.

A paper [19] investigated the impact of shear flexibility and internal viscous friction on the natural frequencies and dynamic amplification factor of a Timoshenko beam made of a viscoelastic material. In [20], the physical sense of the second natural frequency spectrum was clarified using the dimensionless equations of motion for plates incorporating shear deformation and rotational inertia, as well as a parametrical analysis of natural frequencies was carried out. In [21], equations of motion were derived for a general third-order theory with geometric nonlinearity, microstructure dependent size effect, and material gradation. In [22], recent developments in membrane equilibrium finite elements were described, presenting the methodology implemented in a computer programme and demonstrating its application through numerical examples, incorporating thermal and dynamic interactions.

This paper investigates the lowest natural frequencies of unloaded rectangular laminate plates with stacking sequences exhibiting different in-plane and out-plane coupling effects. Hence, in all investigated cases, the B stiffness submatrix is non-zero. The study considers twelve examples of laminate stacking sequences exhibiting different coupling submatrix B types and four cases of calculations using different inertial terms.

The novelty of this study lies in the fact that laminates exhibiting coupling between membrane and bending states have enormous application potential, particularly low-density, thermally stable laminates. The influence of non-zero submatrix elements of stiffness B on the eigenvalue solutions has been examined in detail. This issue is not discussed in the literature from 2015 to 2024 [23–24], yet it is important from a cognitive perspective due to the significant difference in stiffness between plate elements made from general laminates. Only in [25–29] have the authors presented results for selected effects of membrane-bending coupling.

FORMULATION OF THE PROBLEM

According to classical laminate plate theory (CLPT) [30–33], plate materials are subject to Hooke's law. The application of different theories in the analysis of thin-walled laminated plates-namely the FSDT, the S-FSDT – shows that, for length-to-thickness ratios greater than 90, the choice of theory has no significant effect on the solution of the eigenvalue problem [34–37].

CLPT's basic equations of motions resulting from Hamilton's principle are presented in short in Appendix. This study assumes that all investigated laminates have the same ply thickness. According to Equations A.14, we have.

The differential equations of motion (A.10) and (A.15), after considering Equations A.1–A.4, yield a system of three linear differential equations of equilibrium (A.16), expressed as the displacements u, v, w relative to the assumed coordinate system:

$$\begin{gathered}
A_{11}\frac{\partial^2 u}{\partial x^2}+2A_{16}\frac{\partial^2 u}{\partial x\partial y}+A_{66}\frac{\partial^2 u}{\partial y^2}+A_{16}\frac{\partial^2 v}{\partial x^2}+\\
+(A_{12}+A_{66})\frac{\partial^2 v}{\partial x\partial y}+A_{26}\frac{\partial^2 v}{\partial y^2}-B_{11}\frac{\partial^3 w}{\partial x^3}-\\
-3B_{16}\frac{\partial^3 w}{\partial x^2\partial y}-(B_{12}+2B_{66})\frac{\partial^3 w}{\partial x\partial y^2}-B_{26}\frac{\partial^3 w}{\partial y^3}+\\
+[-h\rho_0 u_{,tt}]=0\\
A_{16}\frac{\partial^2 u}{\partial x^2}+(A_{12}+A_{66})\frac{\partial^2 u}{\partial x\partial y}+A_{26}\frac{\partial^2 u}{\partial y^2}+A_{66}\frac{\partial^2 v}{\partial x^2}+\\
+2A_{26}\frac{\partial^2 v}{\partial x\partial y}+A_{22}\frac{\partial^2 v}{\partial y^2}-B_{16}\frac{\partial^3 w}{\partial x^3}-(B_{12}+2B_{66})\frac{\partial^3 w}{\partial x^2\partial y}-\\
-3B_{26}\frac{\partial^3 w}{\partial x\partial y^2}-B_{22}\frac{\partial^3 w}{\partial y^3}+[-h\rho_0 v_{,tt}]=0\\
D_{11}\frac{\partial^4 w}{\partial x^4}+4D_{16}\frac{\partial^4 w}{\partial x^3\partial y}+2(D_{12}+2D_{66})\frac{\partial^4 w}{\partial x^2\partial y^2}+\\
+4D_{26}\frac{\partial^4 w}{\partial x\partial y^3}+D_{22}\frac{\partial^4 w}{\partial y^4}-B_{11}\frac{\partial^3 u}{\partial x^3}-3B_{16}\frac{\partial^3 u}{\partial x^2\partial y}-\\
-(B_{12}+2B_{66})\frac{\partial^3 u}{\partial x\partial y^2}-B_{26}\frac{\partial^3 u}{\partial y^3}-B_{16}\frac{\partial^3 v}{\partial x^3}-\\
-(B_{12}+2B_{66})\frac{\partial^3 v}{\partial x^2\partial y}-3B_{26}\frac{\partial^3 v}{\partial x\partial y^2}-B_{22}\frac{\partial^3 v}{\partial y^3}+\\
+[-h\rho_o w_{,tt}+h^3\rho_2(w_{,xxtt}+w_{,yytt})]=0
\end{gathered}\tag{1}$$

Also, Equation 1 omits the impact of pre-buckling in-plane load, when compared to Equations A.16. This is a standard procedure in free oscillation analysis. A general solution of the system of Equations 1 does not exist. Only two solutions are known for special cases of ply orientations, namely – for regular antisymmetric cross-ply laminate plates and for regular antisymmetric angle-ply laminate plates [30,31]. As far as the general case is concerned, the system in (1) can only be solved in an approximate way.

ANALYSIS OF THE RESULTS

To calculate the lowest natural frequencies of simply supported rectangular laminate plates with the assumed dimensions (L – length, b – width, h – thickness), the system of differential equations in (1) is solved as follows:

$$\begin{gathered}
u=e^{i\omega t}\sum_{n=1}^{N}\sum_{m=1}^{M}U_{mn}\cos\alpha x\sin\beta y\\
v=e^{i\omega t}\sum_{n=1}^{N}\sum_{m=1}^{M}V_{mn}\sin\alpha x\cos\beta y\\
w=e^{i\omega t}\sum_{n=1}^{N}\sum_{m=1}^{M}W_{mn}\sin\alpha x\sin\beta y
\end{gathered}\tag{2}$$

where: $\alpha = m\pi/L$, $\beta = n\pi/b$, ω s the natural frequency of the plate (imaginary part of the eigenvalue), and $i^2 = -1$.

Each single component from the series in Equations 2 corresponds to a general solution for regular antisymmetric cross-ply laminate plates under uniform compression along the 0x axis. In [38] analogous trigonometric functions were assumed along the longitudinal directions. After substituting the predicted solutions of Equations 2 into the system of Equations 1, the linear problem of stability was solved using the Galerkin-Bubnov method [20,30–33]. This method utilizes the orthogonality condition for two functionals: an equilibrium equation functional and a functional of the solution in the area $S=L\,b$. The orthogonality of the two functionals is defined by the equations resulting from variational methods presented in Appendix I. From Equation A.5, after considering Equations A.10, 1 and 2, we ultimately get a linear system of three equations:

$$\begin{gathered}
\int_{t_0}^{t_1}\int_S \begin{Bmatrix} [N_{x,x}+N_{xy,y}] \\ +(-h\rho_0 u_{,tt}) \end{Bmatrix} \cos\left(\frac{r\pi x}{L}\right)\sin\left(\frac{s\pi y}{b}\right) dSdt = 0 \\
\int_{t_0}^{t_1}\int_S \begin{Bmatrix} [N_{y,y}+N_{xy,x}]+ \\ (-h\rho_0 v_{,tt}) \end{Bmatrix} \sin\left(\frac{r\pi x}{L}\right) cos\left(\frac{s\pi y}{b}\right) dSdt = 0 \\
\int_{t_0}^{t_1}\int_S \begin{Bmatrix} [M_{x,xx}+M_{y,yy}+2M_{xy,xy}]+ \\ \begin{bmatrix} -h\rho_0 w_{,tt} \\ +h^3\rho_2\left(w_{,xxtt}+w_{,yytt}\right) \end{bmatrix} \end{Bmatrix} \sin\left(\frac{r\pi x}{L}\right) \\
\sin\left(\frac{s\pi y}{b}\right) dSdt = 0 \\
\text{for } r=1,..R=M;\ s=1,..S=N
\end{gathered} \tag{3}$$

The algebraic system of linear Equations 3 forms a square matrix of the dimensions (3MN). By equating the determinant of this system to zero, we get eigenvalues (i.e. natural frequencies) of the eigenproblem.

Taking into account Equations 2, the constitutive equations Equations A.5 can be written as

$$\begin{aligned}
N_x &= e^{i\omega t}\sum_{n=1}^{N}\sum_{m=1}^{M}\begin{bmatrix} -\alpha A_{11}U_{mn}- \\ \beta A_{12}V_{mn}+ \\ \begin{pmatrix} B_{11}\alpha^2 \\ +B_{12}\beta^2 \end{pmatrix} W_{mn} \end{bmatrix} sin\alpha x\, sin\beta y \\
&+e^{i\omega t}\sum_{n=1}^{N}\sum_{m=1}^{M}\begin{bmatrix} A_{16}(\beta U_{mn}+\alpha V_{mn})- \\ 2\alpha\beta B_{16}W_{mn} \end{bmatrix} cos\alpha x cos\beta y \\
N_y &= e^{i\omega t}\sum_{n=1}^{N}\sum_{m=1}^{M}\begin{bmatrix} -\alpha A_{12}U_{mn}- \\ \beta A_{22}V_{mn}+ \\ \begin{pmatrix} B_{12}\alpha^2 \\ +B_{22}\beta^2 \end{pmatrix} W_{mn} \end{bmatrix} sin\alpha x\, sin\beta y+ \\
&e^{i\omega t}\sum_{n=1}^{N}\sum_{m=1}^{M}\begin{bmatrix} A_{26}\begin{pmatrix} \beta U_{mn}+ \\ \alpha V_{mn} \end{pmatrix}- \\ 2\alpha\beta B_{26}W_{mn} \end{bmatrix} cos\alpha x cos\beta y \\
N_{xy} &= e^{i\omega t}\sum_{n=1}^{N}\sum_{m=1}^{M}\begin{bmatrix} -\alpha A_{16}U_{mn}- \\ \beta A_{26}V_{mn} \\ +\begin{pmatrix} B_{16}\alpha^2 \\ +B_{26}\beta^2 \end{pmatrix} W_{mn} \end{bmatrix} sin\alpha x\, sin\beta y \\
&+e^{i\omega t}\sum_{n=1}^{N}\sum_{m=1}^{M}\begin{bmatrix} A_{66}\begin{pmatrix} \beta U_{mn} \\ +\alpha V_{mn} \end{pmatrix} \\ -2\alpha\beta B_{66}W_{mn} \end{bmatrix} cos\alpha x cos\beta y \\
M_x &= e^{i\omega t}\sum_{n=1}^{N}\sum_{m=1}^{M}\begin{bmatrix} -\alpha B_{11}U_{mn}- \\ \beta B_{12}V_{mn}+ \\ \begin{pmatrix} D_{11}\alpha^2+ \\ D_{12}\beta^2 \end{pmatrix} W_{mn} \end{bmatrix} sin\alpha x\, sin\beta y \\
&+e^{i\omega t}\textstyle\sum_{n=1}^{N}\sum_{m=1}^{M}\begin{bmatrix} B_{16}\begin{pmatrix} \beta U_{mn}\ + \\ \alpha V_{mn} \end{pmatrix} \\ -2\alpha\beta D_{16}W_{mn} \end{bmatrix} cos\alpha x cos\beta y \\
M_y &= e^{i\omega t}\sum_{n=1}^{N}\sum_{m=1}^{M}\begin{bmatrix} -\alpha B_{12}U_{mn}- \\ \beta B_{22}V_{mn} \\ +\begin{pmatrix} D_{12}\alpha^2+ \\ D_{22}\beta^2 \end{pmatrix} W_{mn} \end{bmatrix} sin\alpha x\, sin\beta y \\
&+e^{i\omega t}\sum_{n=1}^{N}\sum_{m=1}^{M}\begin{bmatrix} B_{26}\begin{pmatrix} \beta U_{mn}+ \\ \alpha V_{mn} \end{pmatrix}- \\ 2\alpha\beta D_{26}W_{mn} \end{bmatrix} cos\alpha x cos\beta y \\
M_{xy} &= e^{i\omega t}\sum_{n=1}^{N}\sum_{m=1}^{M}\begin{bmatrix} -\alpha B_{16}U_{mn}- \\ \beta B_{26}V_{mn}+ \\ \begin{pmatrix} D_{16}\alpha^2 \\ +D_{26}\beta^2 \end{pmatrix} W_{mn} \end{bmatrix} sin\alpha x\, sin\beta y \\
&+e^{i\omega t}\sum_{n=1}^{N}\sum_{m=1}^{M}\begin{bmatrix} B_{66}\begin{pmatrix} \beta U_{mn}+ \\ \alpha V_{mn} \end{pmatrix} \\ -2\alpha\beta D_{66}W_{mn} \end{bmatrix} cos\alpha x cos\beta y
\end{aligned} \tag{4}$$

Table 1. Analysed examples of plates made of 18-ply and 16-ply laminates with selected types of coupling effects [39]

Laminate	Stacking sequences of the laminate	Types	Number of laminate layers
EX-1	$[-45/0_5/45/-45/0/(45,-45)_3/-45/45_2]_T$	AsBfDs	18
EX-2	$[-45/45_3/(0,-45)_2/0/45/-45/0/45/-45/45_2/0/-45]_T$	AfBfDf	
EX-3	$[90_{12}/0_6]_T$	AsBLDs	
EX-4	$[90_9/0_9]_T$	AsBLDs	
EX-5	$[90_{15}/0_3]_T$	AsBLDs	
EX-6	$[(45_2,-45_2)_4]_T$	AsBtDs	16
EX-7	$[(0_2,90_2)_4]_T$	AsBLDs	
EX-8	$[0_2,90_2,45_4,-45_4,0_2,90_2]_T$	AsBLtDs	
EX-9	$[45_2,-45_2,90_2,0_2,-45_2,45_2,0_2,90_2]_T$	AsBsDf	
EX-10	$[45_2,-45_2,-45_2,45_2,-45_2,45_2,-45_2,45_2]_T$	AsBtDf	
EX-11	$[45_2,-45_2,-30_2,30_2,-60_2,60_2,-45_2,45_2]_T$	AsBLtDf	
EX-12	$[(0_2,90_2)_2,(-45_2,45_2)_2]_T$	AsBfDf	

It can easily be observed that each of the generalized internal cross-sectional loads in Equations 4 is expressed by two components in the double series, with the first one containing the factor *sinaxsinβy*, and the other *cosαxcosβy*.

This work assumes that the laminate plates are simply supported along their edges for any time *t*. the plates are described by the following boundary conditions:

for $x = 0; L$

$$\int_0^b N_x dy = 0, \quad v{=}0, \quad w{=}0, \quad \int_0^b M_x dy = 0, \tag{5}$$

for *y=0;b*

for $y = 0; b$

$$\int_0^L N_y dy = 0, \quad u{=}0, \quad w{=}0, \quad \int_0^L M_y dy = 0 \tag{6}$$

The boundary conditions in Equations 5a-d, 6a-d) stand for weak boundary conditions for internal loads Equation 4 on the plate edges. It must be emphasized that the first component multiplied by *sinaxsinβy* strictly meets the zeroing condition for a given boundary condition, whereas the other component is equal to zero in integral terms. According to the boundary conditions in Equations A.11 and A.12, for CLPT the weak boundary conditions in Equations 5 and 6 are met. Therefore, the fundamental natural frequencies in (3) are accompanied by internal in-plane loads (4).

For the validation of the employed calculation programme, natural frequencies were determined for regular antisymmetric cross-ply laminate plates [30,31]. Detailed calculations were made for EX-3 (see Table 1 and Case 1 (see Table 2), when: $L/b = 1$, $M=N=1$; $L/b = 1$, $M=N=8$; $L/b = 2$, $M=N=8$. The obtained natural frequencies were then compared with the exact solution [31,31], showing a very good agreement of the results. The Galerkin-Bubnov method was validated for the designed programme. Although a satisfactory agreement was obtained already for $M=N=3$, in further calculations it was taken that $M=N=8$.

This study focused on simply supported rectangular laminate plates of the same dimensions: width b=300 mm, thickness h=2.16 mm, and variable length L =200, 300, 400, 500, 600, 700, 800, 900 mm. The material constants of each layer were assumed to be constant and described by [39]: Young's modulus – 170 GPa, compression modulus – 7.6 GPa, Kirchhoff's modulus - 3.52 GPa, and Poisson's ratio – 0.36, and density ρ = 1500 kg/m^3. Two variants of the laminate were considered [39]: one with 18 plies, each ply having a thickness of 0.12 mm, and the other with 16 plies, each ply having a thickness of 0.135 mm. Given the assumption that all plies are of the same thickness, this yields a case of cross-ply symmetry relative to density, i.e., after Equations A.14), $\rho_1 = 0$.

Table 1 lists twelve examples of general laminates exhibiting selected types of in-plane and out-plane coupling effects [39]. The analysed examples of laminates were denoted by EX-1 through EX-12. In addition, the paper reports the results of four considered cases of calculations. In the first three cases, the calculations were performed using different dynamic terms in the equations of motion in (3) (see Table 2). Case 4 is identical to Case 1, but the B stiffness submatrix is additionally omitted. Figure 1 shows the fundamental natural frequency ω_1 as a function of the dimensionless length L/*b* for all analysed laminate examples (see Table 1), for Case 1 (Table 2).

The fundamental natural frequency ω_1 changes monotonically with an increase in dimensionless length (Figure 1). When the dimensionless length *L/b* equals 0.66, the fundamental natural frequency ω_1 ranges from 1300 to 1700 rad/s for EX-1, EX-2, EX-6/12, and from 800 to 900 rad/s for EX-3 to EX-5. In contrast, when *L/b*=3, the fundamental natural frequency ω_1 ranges from 400 to about 500 rad/s for EX-1, EX-2, EX-6/12, while for EX-3/5 the values range from 350 to 600 rad/s.

Table 2. Cases of calculations made with different dynamic terms and the submatrix B

Case	Equation in Appendix			Comments
	Equation A10.a	Equation A10.b	Equation A10.c	
1		$-h\rho_0 v_{,tt} = 0$	$\rho_2 = 0$	Submatrix B≠0
2	$h\rho_0 u_{,tt} \neq 0$	$-h\rho_0 v_{,tt} \neq 0$	$\rho_2 = 0$	
3	$h\rho_0 u_{,tt} \neq 0$	$-h\rho_0 v_{,tt} \neq 0$	$\rho_2 \neq 0$	
4	$h\rho_0 u_{,tt} = 0$	$-h\rho_0 v_{,tt} = 0$	$\rho_2 = 0$	Submatrix B=0

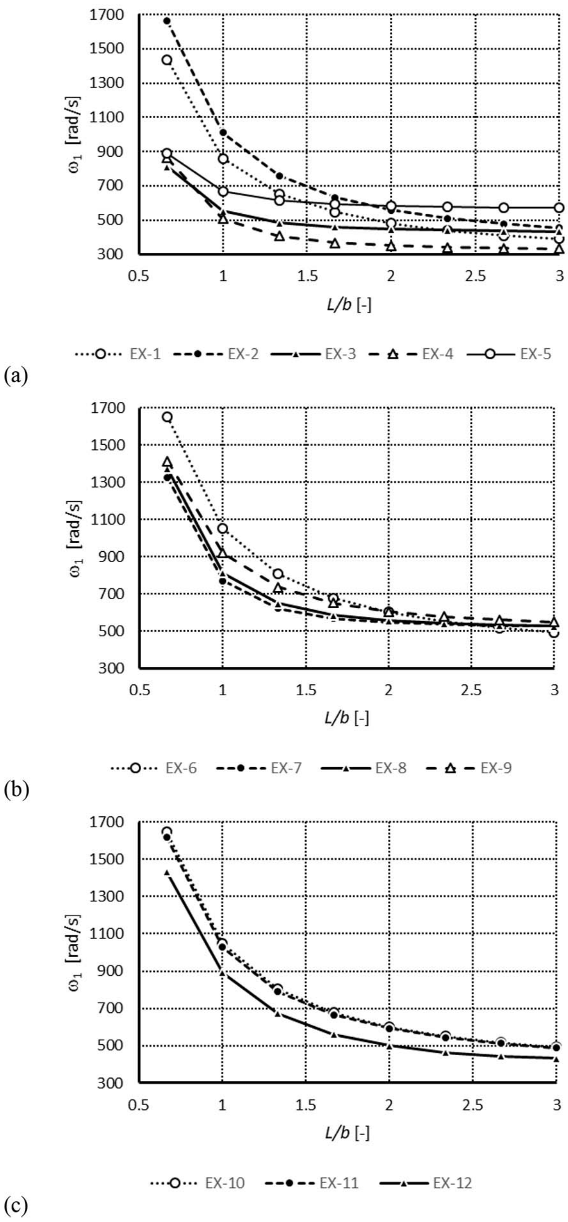

Figure 1. Fundamental natural frequency ω_1 as a function of dimensionless length – case (Table 2): (a) EX-1/5, (b) EX-6/9, (c) EX-10/12

The natural frequency for the second case of calculations (Case 2) is denoted by ω_2, and for the third case (Case 3) by ω_3. For both cases (Cases 2–3), the fundamental natural frequencies decrease when compared to the values obtained in Case 1. The differences are minimal, whatever the dimensionless length L/b. The percentage difference as a function of the dimensionless length L/b is determined as:

$$\delta\omega_i = \frac{(\omega_1 - \omega_i)}{\omega_1} 100\% \tag{7}$$

where: i=2 (Case 2) and i=3 (Case 3).

Figure 2 shows the maximum differences in fundamental natural frequencies (7) that were obtained for all tested plates made of 18-ply and 16-ply laminates (see Table 1). This is the case of EX-1, where the fundamental natural frequency difference (7) does not exceed 0.03%.

Figure 3 shows the percentage differences in natural frequencies for the last variant of the calculations (Case 4 in Table 2), in comparison to Case 1. The percentage deviation as a function of the dimensionless length $\left(\frac{L}{b}\right)$ is expressed as:

$$\delta\omega_4 = \frac{(\omega_1 - \omega_4)}{\omega_1} 100\% \tag{8}$$

where: i=1 (Case 1) and i=4 (Case 4).

A comparison of the results obtained for all laminates, EX-1 through 12 (see Figure 3), reveals that the percentage deviations (Equation 8) are always negative. Omitting the B stiffness matrix always leads to an overestimated value of the fundamental natural frequency. For many laminates, e.g. EX-2, EX-6/11, the difference between fundamental natural frequencies (8) is below 2%. The smallest percentage differences below 1% are obtained for EX-2 (Figure 3(a)), EX-6 (Figure 3(b)), EX-10 (Figure 3(c)), while for the laminates EX-7 through EX-9 (Figure 3(b)), the differences are below 2%. Nonetheless, in extreme cases, the differences exceed dozens percent (EX-3, EX-4, EX-5 in Figure 3(a)). The differences range from -65% to -25% for EX-3, from -62% to -55% for EX4, and from -40% to -5% for EX-5. As the dimensionless length L/b is increased, the fundamental natural frequency differences (8) become practically identical (see EX-2, EX-3, EX-6/11 in Figure 3). Still, one can

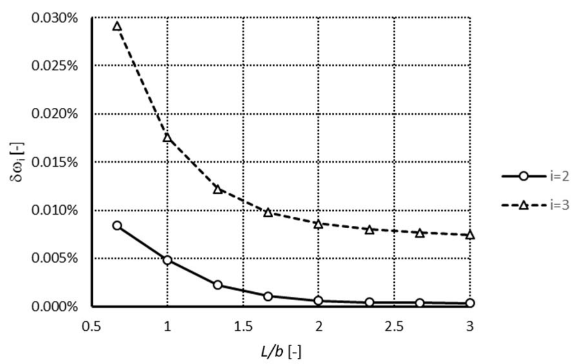

Figure 2. Maximum percentage difference in the fundamental natural frequencies $\delta\omega_2$ and $\delta\omega_3$ (see Equation 7) as a function of dimensionless length (for EX-1)

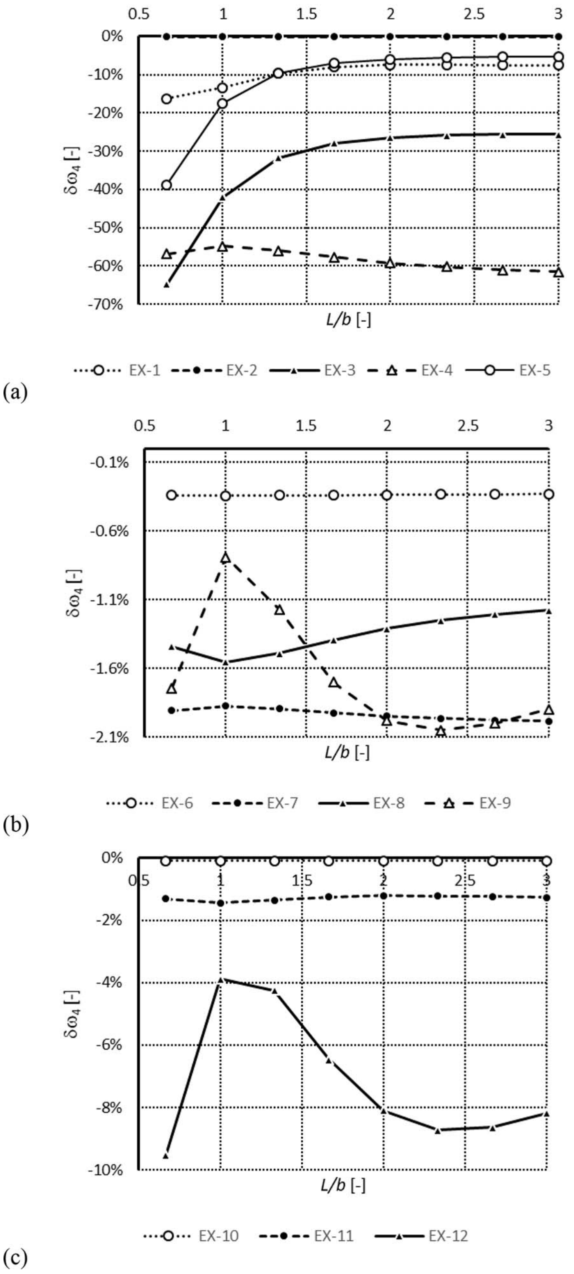

Figure 3. Percentage changes in the natural frequencies $\delta\omega_4 = (\omega_1 - \omega_4) / \omega_1$ as a function of dimensionless length – Case 4 (Table 2): (a) EX-1/5, (b) EX-6/9, (c) EX-10/12

indicate the laminates for which the difference in fundamental natural frequencies (8) significantly depends on the dimensionless length L/b (EX-1, EX-3, EX-5 in Figure 3(a)). For EX-7-EX-9, EX-11, EX-12, one can observe a rapid change in the percentage difference of natural frequencies as a function of dimensionless length, which may be related to a change in the number of half waves describing the natural frequency when B=0.

To verify presented analytical-numerical model (ANM), numerical simulations were performed by the finite element method (FEM) using the commercial software Abaqus. A shell model was created using S4R type shell finite elements of 5 mm in size (i.e. 4-node doubly curved thin or thick shell, reduced integration, hourglass control, finite membrane strains).

The simply supported boundary conditions were implemented such that all plate edges were restrained against displacement in the normal direction, while one edge was additionally constrained against in-plane motion. The stacking sequence of laminate plies in the FEM model was defined in the Composite Layup Manager module separately for each ply by defining the mechanical properties, thickness and orientation of each ply in the coordinate system.

The eigenproblem was solved by determining the lowest natural frequency and corresponding eigenmode with the use of the SUBSPACE algorithm. The FEM model was validated by assessing the influence of element type and mesh density, refining the boundary conditions to accurately represent simply supported edges, and verifying the algorithms used to solve the eigenvalue problem.

Table 3 lists the lowest natural frequencies obtained with the both calculation methods, and their deviations are given in brackets. Excellent agreement between the results can be observed. The relative differences of the lowest natural frequencies values calculated by the both methods are lower than 3%.

A comparison of the percentage differences in fundamental natural frequencies (see Figure 3) demonstrates that the greatest differences are observed EX-3, EX-4, and EX-5 with regular cross-ply laminate plates [30, 31] and the AsBLDs coupling effect. For the coupling submatrix, we have $B_{11}>0$ and $B_{11}=-B_{22}$, while other elements of this submatrix are equal to zero. For EX-3 and EX-4, the absolute values of B_{11} and B_{22} are higher than those obtained for the bending stiffness components D_{ij}, which is the only such case known to the authors. For EX-5, $B_{11}<D_{11}$, $B_{11}<D_{22}$ and $D_{11}<D_{22}$. In [40], the authors introduced dimensionless reduction factors for a 1D beam model, defined as:

$$\alpha_1 = 1 - \frac{(B_{11})^2}{A_{11}D_{11}} \qquad \alpha_2 = 1 - \frac{(B_{22})^2}{A_{22}D_{22}} \qquad \alpha_6 = 1 - \frac{(B_{66})^2}{A_{66}D_{66}} \tag{9}$$

in the $0x$, $0y$ and $0z$ direction, respectively.

Table 3. Lowest natural frequencies in rad/s and their relative differences in % given in brackets

Laminate	*L/b*=1		*L/b*=2		*L/b*=3	
	ANM*	FEM	ANM*	FEM	ANM*	FEM
EX-1	859(3%)	885	482(2%)	470	391(2%)	382
EX-2	1010(1%)	997	557(1%)	553	455(1%)	453
EX-3	553(1%)	559	447(0%)	448	435(0%)	435
EX-4	508(1%)	514	350(0%)	352	333(0%)	333
EX-5	669(0%)	671	583(0%)	583	573(0%)	573
EX-6	1052(2%)	1031	602(1%)	594	494(1%)	489
EX-7	772(1%)	778	547(0%)	548	527(0%)	527
EX-8	812(3%)	791	557(3%)	543	526(2%)	515
EX-9	920(2%)	906	606(0%)	607	550(0%)	552
EX-10	1048(3%)	1022	601(2%)	590	493(1%)	487
EX-11	1027(1%)	1016	592(1%)	585	489(1%)	484
EX-12	892(3%)	870	499(1%)	496	433(1%)	430

Note: *Presented method.

It must be emphasized that the ratio $\frac{(B_{ii})^2}{A_{ii}D_{ii}}$ is dimensionless. Table 4 lists the values of the above reduction factors Eq.(9) for all considered laminates, EX-1 through EX-12. For EX-3, the dimensionless reduction factors are $\alpha_1 = 0.262$, $\alpha_2 = 0.633$, and $\alpha_6 = 1.0$ (Table 3). For EX-4, $\alpha_1 = \alpha_2 = 0.373$, where $\alpha_6 = 1.0$ and its value does not change. For EX-5, $\alpha_1 = 0.320$, $\alpha_2 = 0.905$, which is the highest value compared to EX-3 and α_6 EX-4, and $\alpha_6 = 1.0$. To the knowledge of the authors of this paper, there exists no other case when the reduction factor is lower than 0.5 for α_1. Hence, the considerable increase in natural frequency. The second highest percentage difference for Case 4 is EX-1, exhibiting the in-plane and out-plane coupling effect of AsBfDs type. The reduction factors are respectively $\alpha_1 = 0.837$, $\alpha_1 = 0.876$, and $\alpha_6 = 0.843$ (Table 4). The values of α_1 and α_2 are significantly higher than those obtained for EX-3. It is noteworthy that the coupling stiffness submatrix B contains all non-zero components. B_{11} has the highest absolute value, which is about 3 times higher than that of a successive component in the B submatrix. In addition, $B_{11}<0$, while all other components are greater than zero.

The third case was the laminate EX-12 with a coupling of AsBfDf type. For this case, all components of the coupling stiffness and the bending stiffness submatrix differ from zero. The factors are respectively $\alpha_1 = 0.885$, $\alpha_2 = 0.981$, and $\alpha_6 = 0.459$ (Table 4). As it can be seen, the reduction factor for shear/torsion is lower than 0.5. This leads to a several percent decrease in the difference between the natural frequencies for this case.

Summing up, the lowest reduction factors for a 1D beam model Equation 7 were obtained – in an ascending order – for the following laminates: EX3-EX-5, EX-1, and EX-12. This explains the above-mentioned impact on the percentage differences between the natural frequencies obtained in Case 4 for the tested laminates.

The calculations of the eigenproblem of the laminate rectangular plates show that for the correct determination of the impact of the coupling submatrix components, one must perform a detailed analysis of all stiffness matrix components and reduction factors for a 1D beam model. It should be remembered that the mere consideration of the coupling stiffness submatrix B never leads to reduced natural frequencies.

Table 4. Dimensionless reduction factors α_1, α_2 and α_6 Equations 9 for the laminates under consideration

Laminate	α_1	α_2	α_6
EX-1	0.837	0.876	0.843
EX-2	0.998	0.999	0.999
EX-3	0.262	0.633	1.0
EX-4	0.373	0.373	1.0
EX-5	0.320	0.905	1.0
EX-6	1.0	1.0	1.0
EX-7	0.961	0.961	1.0
EX-8	0.987	0.987	1.0
EX-9	0.980	0.987	0.865
EX-10	1.0	1.0	1.0
EX-11	0.972	0.972	1.0
EX-12	0.885	0.981	0.459

CONCLUSIONS

The study considered the fundamental natural frequencies of rectangular laminate plates with the full ABD stiffness matrix, with particular emphasis on in-plane and out-plane coupling effects. The plates under study were made of laminates with different stacking sequences exhibiting different coupling effects. The plates were assumed to be simply supported along all edges. The considerations were limited to the case of general thermostable laminates. Particular attention was paid to the non-zero coupling stiffness submatrix B. Variable plate length and ply stacking sequence, as well as four variants of the influence of dynamic terms, were investigated in terms of their impact on fundamental natural frequencies.

The fundamental natural frequencies of the short plates increase to a considerable extent because the boundary conditions make them significantly stiffened. In the long plates, this effect disappears and the frequencies decrease rapidly.

The omission of the B stiffness matrix always leads to an overestimated fundamental natural frequency. In many cases, the differences between fundamental natural frequencies are small. However, in extreme cases, these differences exceed several dozen percent. With an increase in dimensionless length, the fundamental natural frequency differences can become practically identical. Nonetheless, it is possible to identify laminates where the fundamental natural frequency difference significantly depends on the dimensionless length value, which may correspond to a change in the number of half-waves describing the lowest eigenmode, when B=0.

The inclusion of different dynamic terms in the equations of motion for the tested laminate plates was of secondary importance. A decrease in the fundamental natural frequencies was observed, but the differences were minimal whatever the dimensionless length value.

REFERENCES

1. Rastgaar Aagaah M., Mahinfalah M., Nakhaie Jazar G. Natural frequencies of laminated composite plates using third order shear deformation theory. Composite Structures, 2006, 72, 273–279.
2. [S, Wang K.M., Ai Y.T., Sha Y.D, Hong Shi H. Natural frequencies of generally laminated composite plates using the Gaussian radial basis function and first-order shear deformation theory. Thin-Walled Structures, 2009, 47, 1265–1271.
3. Jin G., Ye T., Su Z. Structural Vibration. A uniform accurate solution for laminated beams, plates and shells with general boundary conditions. Science Press, Beijing and Springer-Verlag Berlin Heidelberg, 2015.
4. Luo Y., Hong M., Liu Y. Analytical solutions to the fundamental frequency of arbitrary laminated plates under various boundary conditions. J. Marine Sci. Appl., 2015, 14, 46–52.
5. Papkov S.O., Banerjee J.R. A new method for free vibration and buckling analysis of rectangular orthotropic plates. Journal of Sound and Vibration, 2015, 339, 342–358.
6. Li D., York C.B. Bounds on the natural frequencies of laminated rectangular plates with extension-twisting (and shearing–bending) coupling. Composite Structures, 2015, 131, 37–46.
7. Li D., York C.B. Bounds on the natural frequencies of laminated rectangular plates with Extension–Bending coupling. Composite Structures, 2015, 133, 863–870.
8. Sayyad A.S., Ghugal Y.M. On the free vibration analysis of laminated composite and sandwich plates: A review of recent literature with some numerical results. Composite Structures, 2015, 129, 177–201.
9. Abedi M., Jafari-Talookolaei R-A., Valvo P.S. A new solution method for free vibration analysis of rectangular laminated composite plates with general stacking sequences and edge restraints. Computers and Structures, 2016, 175, 144–156.
10. Muni Rami Reddy R., Karunasena W., Lokuge W. Free vibration of functionally graded-GPL reinforced composite plates with different boundary conditions. Aerospace Science and Technology, 2018, 78, 147–156.
11. Sinhaa L., Mishraa S.S., Nayaka A.N., Sahub S.K. Free vibration characteristics of laminated composite stiffened plates: Experimental and numerical investigation. Composite Structures, 2020, 233, 111557.
12. Narita Y., Michio Innami M. Identifying all combinations of boundary conditions for in-plane vibration of isotropic and anisotropic rectangular plates. Thin-Walled Structures, 2021, 164, 107320.
13. Mohamed S.A, Mohamed N., Eltaher M.A. Bending, buckling and linear vibration of bio-inspired composite plates. Ocean Engineering, 2022, 259, 111851.
14. Guo Q., Shi G. An accurate and efficient 4-noded quadrilateral plate element for free vibration analysis of laminated composite plates using a refined third-order shear deformation plate theory. Composite Structures, 2023, 324, 117490.
15. Li M., Soares C.G., Liu Z., Zhang P. Free and forced vibration analysis of carbon/glass hybrid composite laminated plates under arbitrary boundary conditions. Applied Composite Materials, 2024, 31, 1687–1710.

16. Bisheh H. Free vibration analysis of smart laminated bamboo fibre-reinforced composite plates under different boundary conditions. Structures, 2025, 79, 109384.
17. Syed F.H., Thong L.W., Baig M.F., Yee Kit Chan, Ervina Efzan M.N. A comparative study of material and structural configurations in piezoelectric energy harvesting. Emerging Science Journal 2025, 9(1), 346–361. https://doi.org/10.28991/ESJ-2025-09-01-019
18. Chitaoui H., Megnounif A., Benadla Z. Optimal placement of vibration control systems in a smart civil engineering structure. Civil Engineering Journal 2025, 11(8), 3495–3515. https://doi.org/10.28991/CEJ-2025-011-08-022
19. Manevich A. Kolakowski Z. Free and forced oscillations of Timoshenko beam made of viscoelastic material. J. Theor. Appl. Mech., 2011; 49(1), 3–16.
20. Manevich A.I., Kolakowski Z. Revisiting the theory of transverse vibrations of plates with shear deformation, International Applied Mechanics, 2014, 50(2), 196–205.
21. Reddy J.N., Kim J. A nonlinear modified couple stress-based third-order theory of functionally graded plates. Compos Struct 2012, 94(3), 1128–1143.
22. Ramsay A., Maunder E. Equilibrium finite element membranes with body loads. Academia Engineering 2024, 1. https://doi.org/10.20935/AcadEng7459
23. Wang J., Chang Z., Liu T., Chen L. A review of linear and nonlinear vibration analysis of composite laminated structures by computational approaches: 2015–2024 Nonlinear Dyn 2025, 113, 10839–10859. https://doi.org/10.1007/s11071-024-10837-y
24. Sayyad A.S., Ghugal Y.M. Bending, buckling and free vibration of laminated composite and sandwich beams: A critical review of literature. Composite Structures 2017, 171, 486–504. http://dx.doi.org/10.1016/j.compstruct.2017.03.053
25. Li Y., Xing Y. Analytical solutions for the free vibration of rectangular laminated thin plates. Composite Structures 2026, 385(1), 120215. https://doi.org/10.1016/j.compstruct.2026.120215
26. Abedi M., Jafari-Talookolaei R.-A., Valvo P.S. A new solution method for free vibration analysis of rectangular laminated composite plates with general stacking sequences and edge restraints Computers and Structures 2016, 175, 144–156. http://dx.doi.org/10.1016/j.compstruc.2016.07.007
27. Wang W., Wang Q., Zhong R., Chen L., Shi X. Stacking sequence optimization of arbitrary quadrilateral laminated plates for maximum fundamental frequency by hybrid whale optimization algorithm Composite Structures 2023, 310, 116764. https://doi.org/10.1016/j.compstruct.2023.116764
28. Cui D., Zhang M., Li D. Design of carbon fiber-reinforced composite laminates with near-zero coefficient of thermal expansion and extension-twisting coupling. Composites Communications 2025, 59, 102564. https://doi.org/10.1016/j.coco.2025.102564
29. Cui D., Li D., Zhou S. Solution of coupled mechanical behavior of bending-twisting coupled box structure based on multi-coupled laminates. Composite Structures 2022, 301, 116202. https://doi.org/10.1016/j.compstruct.2022.116202
30. Jones R.M. Mechanics of Composite Materials. 2nd, Ed. Taylor & Francis, London, 1999.
31. Jones R.M. Buckling of Bars, Plates, and Shells. Bull Ridge Publishing, Blacksburg, Virginia, 2006.
32. Kołakowski Z., Kowal-Michalska K. (Eds.) – Statics, dynamics and stability of structural elements and systems, Vol. 2, Statics, dynamics and stability of structures, Technical University of Lodz, A series of Monographs, Lodz 2012, 499.
33. Kowal-Michalska K. (Ed.). Dynamic stability of composite plate structures /in Polish/. WNT Foundation for Scientific and Technical Books, Warsaw, 2007, p.172.
34. Kolakowski Z., Jankowski J., Some inconsistencies in nonlinear buckling plate theories — FSDT, S-FSDT, HSDT, Materials, 14(9), 2021, 2154. https://doi.org/10.3390/ma140902154
35. Kołakowski Z., Królak M. Modified continuity conditions of plates in beam-column using the Mindlin plate theory, Thin-Walled Structures, 2014, 74, 261–268.
36. Kołakowski Z., Jankowski J. Effect of membrane components of transverse forces on magnitudes of total transverse forces in the nonlinear stability of plate structures. Materials 2020, 13(22), 5262. https://doi.org/10.3390/ma13225262
37. Kolakowski Z., Jankowski J. Some inconsistencies in the nonlinear buckling plate theories — FSDT, S-FSDT, HSDT. Materials 2021, 14(9), 2154. https://doi.org/10.3390/ma1 4092154
38. Kolakowski Z., Krolak M. Modal coupled instabilities of thin-walled composite plate and shell structures. Composite Structures, 2006, 76, 303–313.
39. Teter A., Kolakowski Z. Susceptibility versus flexural stiffness in the stability of hybrid laminate columns with a rectangular cross section for a 1D model. Composite Structures 2024, 345, 118362.
40. Teter A., Mania R.J., Kołakowski Z. Non-linear stability and load-carrying capacity of thinwalled laminated columns in aspects of coupled buckling and coupled stiffness submatrix. Composite Structures, 2018, 192, 72–81.